



MINISTRY OF TECHNOLOGY

AERONAUTICAL RESEARCH COUNCIL

CURRENT PAPERS

The Pressure Drag of an Aerofoil with  
Six Different Round Leading Edges;  
at Transonic and Low Supersonic Speeds

By

Information Centre  
DRA Bedford

P. G. Wilby

LONDON: HER MAJESTY'S STATIONERY OFFICE

1967

FIVE SHILLINGS NET



January, 1966

The Pressure Drag of an Aerofoil with  
Six Different Round Leading Edges, at  
Transonic and Low Supersonic Speeds

- By -

P. G. Wilby

---

SUMMARY

The experimental pressure drags of a two-dimensional aerofoil are compared, for a wide range of leading-edge radii and other variations in curvature distribution, at transonic and low supersonic speeds. It is found that the drag does not increase with increasing leading-edge radius if the profile is designed so as to generate a rapid supersonic expansion. Furthermore, for a given radius, significant reductions in drag can be achieved by changing the way in which the leading-edge circle blends into the overall profile.

---

Notation

$C_D$	pressure drag coefficient
$C_L$	lift coefficient
$c$	aerofoil chord length
$H$	total pressure
$M$	Mach number
$p$	static pressure
$r$	surface radius
$z$	aerofoil ordinate defined in Section 4.
$\alpha$	angle of incidence

y/

$\gamma$  ratio of specific heats of air

$\theta$  surface slope

### Subscripts

$\infty$  free-stream value

$o$  stagnation value

## 1. Introduction

It has been pointed out by Graham<sup>1</sup> that the pressure drag of a two-dimensional aerofoil is not necessarily increased by blunting the leading edge. Graham measured the drag of a circular arc biconvex aerofoil, first with the leading edge sharp and then cut back in stages to form circular profiles with increasing radius. Although the surface slope was continuous for these aerofoils, there was a discontinuity in curvature where the profile changed from the small leading-edge circle to the large circle of the basic profile. He found, as expected, that the high pressure region in the immediate vicinity of the stagnation point extended as the leading-edge radius increased, but that the effect of this on drag was offset by the suction generated over the outer parts of the blunt leading edges. However, the particular profile considered by Graham was of a simple geometric shape and possessed features that may be undesirable in a wing section. The large curvature discontinuity could cause flow separation under certain conditions, especially at low speeds, and the suction peaks generated at high subsonic speeds were too high. This led to a premature drag rise rather than the delayed drag rise that can be obtained with optimum "peaky" aerofoils.

With this in mind, the transonic and supersonic drags will be examined here for an aerofoil with six variations of leading-edge shape, each of which was intended to retain acceptable characteristics at low speeds and high subsonic speeds. In fact, the basic aerofoil was designed as a practical wing section with an emphasis on good transonic behaviour.

## 2. Aerofoil and Leading-Edge Profiles

The basic aerofoil has a maximum thickness of 6.5% chord at about 40% chord from the leading edge, and the leading edges are shown in Fig. 1. Profiles 1, 2, 3 and 4 are identical aft of 10% chord but profile 6 differs over the first 20% of chord. Profile 5 has the same leading-edge circle as 3 but its upper surface is lowered and does not blend with the basic aerofoil until 40% chord is reached (as shown in Fig. 2). All aerofoils except 4 and 6 have the same chord length, the two exceptions being slightly extended.

All but one (No. 4) of the profiles are of the "peaky" type in that they generate a rapid expansion round the leading edge itself followed by a compression on the downstream surface. Their leading edges are circular with the constant, high curvature retained until the surface slope falls to about 30° to the chord line, at which point there comes a rapid decrease to low values of curvature. The surface slope is everywhere continuous. Apart from the

differences/

AERONAUTICAL RESEARCH COUNCIL

Publications Section,  
National Physical Laboratory,  
Teddington, Middlesex.

*T. G. Wilby, Esq.*

*10/4/67.*

Dear Sir,

I enclose ten copies of Current Paper No. *921*  
for your retention. Please sign and return the attached form of  
receipt.

Yours faithfully,

*A. S. Soden (Miss)*

for Publications Officer

---

The Publications Officer,  
Aeronautical Research Council,  
National Physical Laboratory,  
Teddington, Middlesex.

I hereby acknowledge receipt of ten copies of Current  
Paper No. . . *921*.

Date . . . . .

Signed . . . . .



differences in leading-edge radii, the profiles differ in the way in which the rapid curvature change takes place, as is shown by Figs. 3 and 4, where curvature is plotted against surface slope. The initial curvature change for profiles 1 and 6 is almost discontinuous whereas that for 2, 3 and 5 is more gradual. For profiles 2 and 3 there is a sharp corner in the curvature distribution at the foot of the rapid change, but this has been smoothed out for profile 5.

Profile 4 represents a more conventional type of aerofoil. It has a non-circular leading edge (Fig. 3) which does not generate a suction peak and has the smallest leading-edge radius. The comparison of drags of this aerofoil with those of the "peaky" aerofoils is thus of special interest in the present context.

### 3. A Brief Outline of the Factors Governing the Formation of Supersonic Suction Peaks

The idea of a "peaky" type of velocity distribution, as introduced by Pearcey<sup>2</sup>, is that a rapid supersonic expansion should be generated at the leading edge, halted at the appropriate level and followed immediately by an isentropic compression. A region of sustained high curvature at the leading edge provides the required degree of flow deflection that causes the expansion. This expansion terminates when a large and rapid drop in curvature occurs. If the curvature drop is sufficiently large then the compression waves that have been reflected from the sonic line will be stronger than the expansion waves generated by the surface, and a net compression results on the aerofoil surface. A suction peak is thus formed at the abrupt change of curvature. The exact form of the curvature distribution, at and after the curvature change, is very important in controlling the rate of the compression and the isentropic nature of the flow. Even when a shock wave does form, its strength can be minimised by a well designed curvature distribution.

A circular leading edge is an effective way of achieving the rapid expansion, and obviously, the longer the profile stays with the circle, the larger will be the expansion. Now if the circle is maintained sufficiently far to give a large expansion, the surface slope will have reached such a small value that a rapid change to a low surface curvature will be necessary to blend the circular leading edge with a practical aerofoil profile. Hence, this type of leading edge leads automatically to the features essential to the peaky velocity distribution.

The magnitude of the suction peak will depend upon the change in surface slope between the stagnation point and the point of minimum pressure. If we consider the minimum pressure point to be fixed by the geometry of the aerofoil, then the level of the minimum pressure will be varied by moving the stagnation point, and this is of course done by a change of incidence. At the Mach numbers considered here, the point of minimum pressure, or peak position, is found to lie towards the foot of the rapid curvature change, and is at a lower value of surface slope for profiles 2, 3 and 5 than for profiles 1 and 6. Thus, we can expect that the peak generated by profiles 2, 3 and 5 will be higher than those generated by 1 and 6.

For an aerofoil of given thickness and chord, with a circular leading edge, it is possible for the profile to stay with the circle to a lower value of

surface/

surface slope as the leading-edge radius becomes progressively larger. If this possibility is exploited, then the larger the radius becomes, the larger will be the suction peak. From the point of view of supersonic drag, the increased suction peak tends to counter the effect of the increased bluntness. However, a very high suction peak may not be acceptable at subsonic speeds, as mentioned earlier, and because of this, the peak of profile 2 was kept below the possible maximum for an aerofoil with such a large leading-edge radius.

#### 4. Measurement of Pressure Drag

Two-dimensional models with a chord length of 5 in. (127 mm) were tested in the 20 in. x 8 in. (508 mm x 203 mm) wind tunnel at the N.P.L. The models were provided with static pressure holes drilled normal to the surface, and pressure distributions were measured by a multi-tube manometer. Boundary-layer transition was induced by a carborundum band at the leading edge.

The pressure drag coefficient  $C_D$  was given by a graphical evaluation of the equation

$$C_D = \frac{2}{\gamma M_\infty^2} \frac{H_0}{p_\infty} \int_{\frac{z}{c} \min}^{\frac{z}{c} \max} \Delta \left( \frac{p}{H_0} \right) d \left( \frac{z}{c} \right),$$

where  $\Delta$  denotes the difference between pressures at points with the same value of  $z/c$ . For this purpose, the ratio  $p/H_0$  of static pressure to stagnation pressure was plotted against the ordinate  $z$  divided by the aerofoil chord  $c$ .  $z$  was the perpendicular distance, of a point on the aerofoil surface, from a line passing through the trailing edge in a direction parallel to the free stream. Thus, the pressure difference between two elements on the surface with equal values of  $z$  represents a direct contribution to the drag.

The forms taken by the above type of pressure plot, and their interpretation in analysing the sources of pressure drag, have been discussed by Pearcey<sup>2</sup> and Graham<sup>1</sup>. Typical examples for the cases studied here are annotated in Figs. 6 and 7 in order to assist in their interpretation.

Attention is confined to pressure drag and the discussion relates to the effects of leading-edge shape on wave drag, on the assumption that the changes in leading-edge shape do not influence the boundary-layer contribution to the pressure drag. That this assumption is valid is indicated by the fact that the pressures at the rear of the aerofoil were never materially affected by the leading-edge changes.

#### 5. Comparison of Pressure Drags for $M_\infty = 1$ and $1.4$

The values of pressure drag for the various profiles will be considered first at those Mach numbers for which the changes are due to differences in the fully established wave drag, that is, at and beyond the "transonic hump".

Values of  $C_D$  at  $M_\infty = 1$  are plotted against  $C_L$  in Fig. 5. At low  $C_L$  all the profiles have almost the same drag, but as  $C_L$  increases then

the/



the spread of  $C_D$  values increases. However, over the range of  $C_L$  considered, the drags of profiles 1, 2, 3 and 4 can be taken to be alike, with the drag of profile 6 slightly higher and that of profile 5 somewhat lower. It is not possible to relate drag directly to leading-edge radius and it is of interest to look at a few typical pressure distributions.

In Fig. 6 we have pressure distributions for profiles 2, 3 and 4 at  $\alpha = 0^\circ$ . These profiles represent the full range of leading-edge radii and it is immediately seen how the suction peaks eat into the drag area and so offset the extra fullness at the immediate leading edge. A similar situation is found in Fig. 7 for aerofoils at  $3^\circ$  incidence.

Fig. 8 demonstrates that the way in which the leading-edge circle blends into the basic aerofoil can be important. Here, pressure distributions for profiles 3 and 5 are compared; these two differ on leaving the leading-edge circle. The curvature of profile 5 is such as to reduce the pressure rise that follows the suction peak to such an extent that the area of the drag loop to the right of the peak for profile 3 is eliminated, and in fact replaced by a very small suction loop.

The profiles with the highest and lowest drags have their pressure distributions compared in Fig. 9. This shows clearly how it comes about that the profile with the larger leading-edge radius has the lower drag.

A Mach number of 1.4 produces much the same pattern of results, and  $C_D$  is plotted against  $C_L$  in Fig. 10. Profiles 2 and 6 which have the largest and smallest "peak"-producing leading-edge radii have the same drag, and their pressure distributions are compared in Fig. 11. The profiles with the highest and lowest drags are 1 and 5 respectively and their pressure distributions are compared in Fig. 12. As these two profiles have almost the same leading-edge radii, the importance of the blending from circle to basic profile is apparent.

With regard to the level of drag at zero lift and  $M_\infty = 1$ , it is interesting to note that the theoretical pressure drag coefficient<sup>1</sup> for a biconvex circular arc section (sharp leading edge) of the same thickness chord ratio as that of the present aerofoils, has the value 0.038. This, as is seen in Fig. 5, is almost identical with the aerofoils considered here.

## 6. Comparison of Pressure Drags at Subsonic Speeds

A comparison of the pressure distributions and their associated drags is a little less straightforward at subsonic speeds. In inviscid shock-free flow the thrust and drag loops, such as those in Fig. 13, would exactly balance to give the zero drag for potential flow, in spite of substantial differences in the shape of the loops for the different leading-edge shapes.

In practice each aerofoil will have a finite pressure drag, even in the absence of shock waves, because the boundary-layer growth will prevent the realisation of true potential flow. It then becomes instructive to examine how pressure drag is augmented by the development of shock wave drag as Mach number is increased, and how this development differs according to leading-edge shape. (Pearcey<sup>2</sup> has shown that all the initial increase in wave drag can be traced to changes in the thrust loop.) Profiles 4 and 5 provide contrasting

examples/

examples of pressure-distribution development with increasing Mach number, as illustrated in Figs. 13 to 15.

In Fig. 13 we have the two different types of pressure distribution compared at a subcritical Mach number and it is seen that both profiles have the same drag. The situation at  $M_\infty = 0.7$  is shown in Fig. 14, and here shock waves have appeared and the drag of both profiles has risen slightly. It is noticed the drag of the profile 5 is slightly higher than that of the non-peaky aerofoil, and this is due to the strong shock which sits ahead of the crest of profile 5. This situation can be improved by changing the shape of the aerofoil to one more like profile 3, whose pressure distribution is also shown. Due to its improved pressure distribution which effectively eliminates wave drag, profile 3 is found to have less drag than either of the other two.

When Mach number has increased to 0.8 the pressure distributions of profiles 4 and 5, as shown in Fig. 15, provide an interesting contrast. Here we see that profile 5 still retains a suction loop (though somewhat reduced in area) due to the "peaky" nature of its pressure distribution, whereas the suction loop for profile 4 has now become an extension of the drag loop. The result is that at this Mach number the drag of profile 5 is considerably less than that of profile 4.

## 7. Conclusions

It has been shown that an increase of leading-edge radius is not necessarily accompanied by an increase of drag. Although an aerofoil with a large leading-edge radius has a large frontal area in the high pressure region, this can be balanced by a low pressure region which results from the large and rapid expansion that can be generated by the blunt leading-edge. This confirms the conclusions reached by Graham<sup>1</sup>, but here we have considered a practical wing section.

The importance of designing the blunted aerofoil to generate and exploit the low pressure region has been indicated, and it has been shown to be possible to produce an aerofoil with a large leading-edge radius which has less drag than one with a more conventional and considerably smaller leading-edge radius.

---

References/

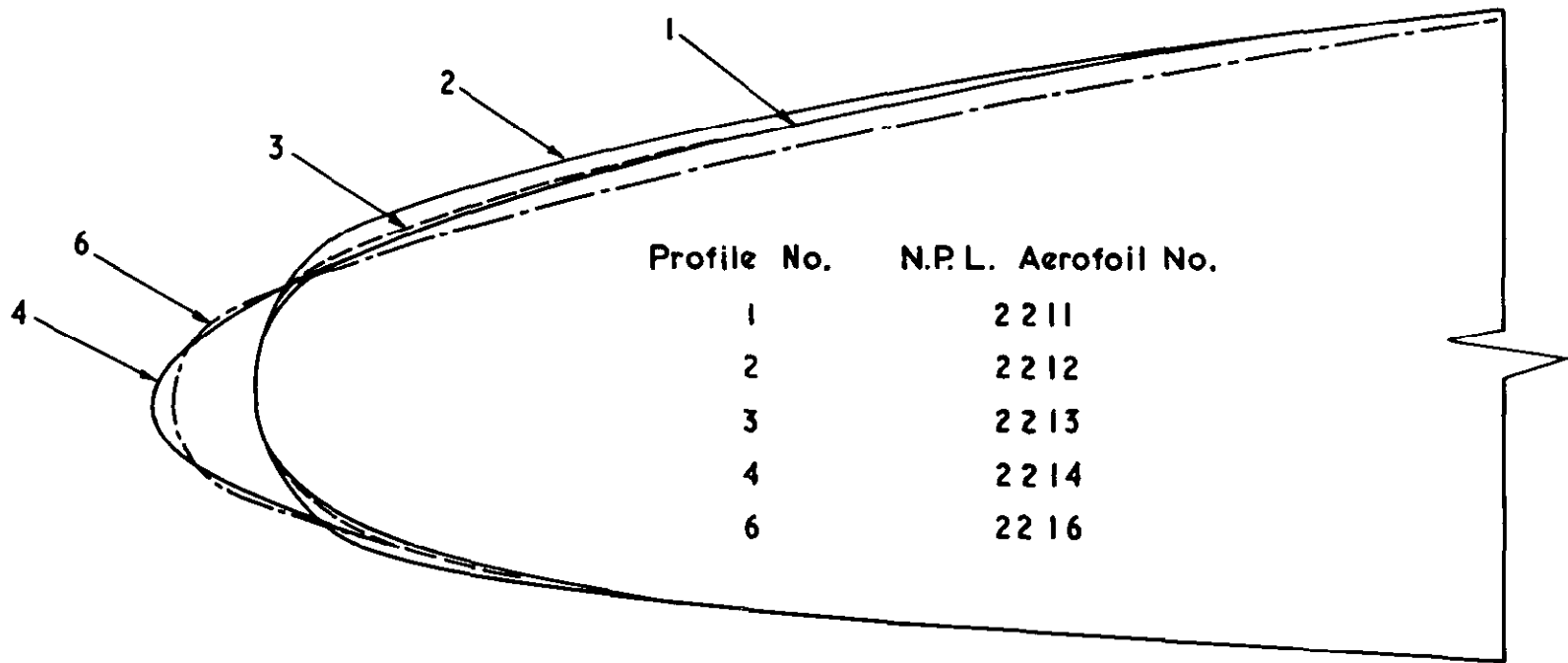
References

<u>No.</u>	<u>Author(s)</u>	<u>Title, etc.</u>
1	W. J. Graham	The pressure drag due to blunt leading edges on two-dimensional aerofoils, at transonic and low supersonic speeds. A.F.C. R. & M. 3465. May, 1965.
2	H. H. Pearcey	The aerodynamic design of section shapes for swept wings. Advances in Aeronautical Sciences, Vol.3. Proceedings of the Second International Congress in the Aeronautical Sciences Zürich 12-16 September, 1960. Pergamon Press Ltd., pp.277 - 322, 1962.
3	J. R. Spreiter and A. Y. Alksne	Thin aerofoil theory based on approximate solution of the transonic flow equation. NACA TN 3970, 1958.

---

DS.



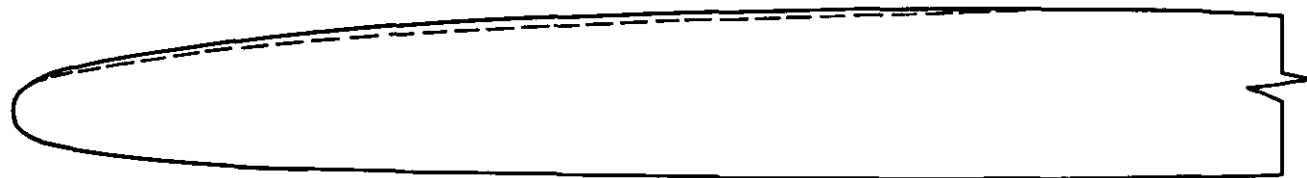


Profile No.	N.P.L. Aerofoil No.
1	2211
2	2212
3	2213
4	2214
6	2216

Leading edge profiles (0 to 10% chord)

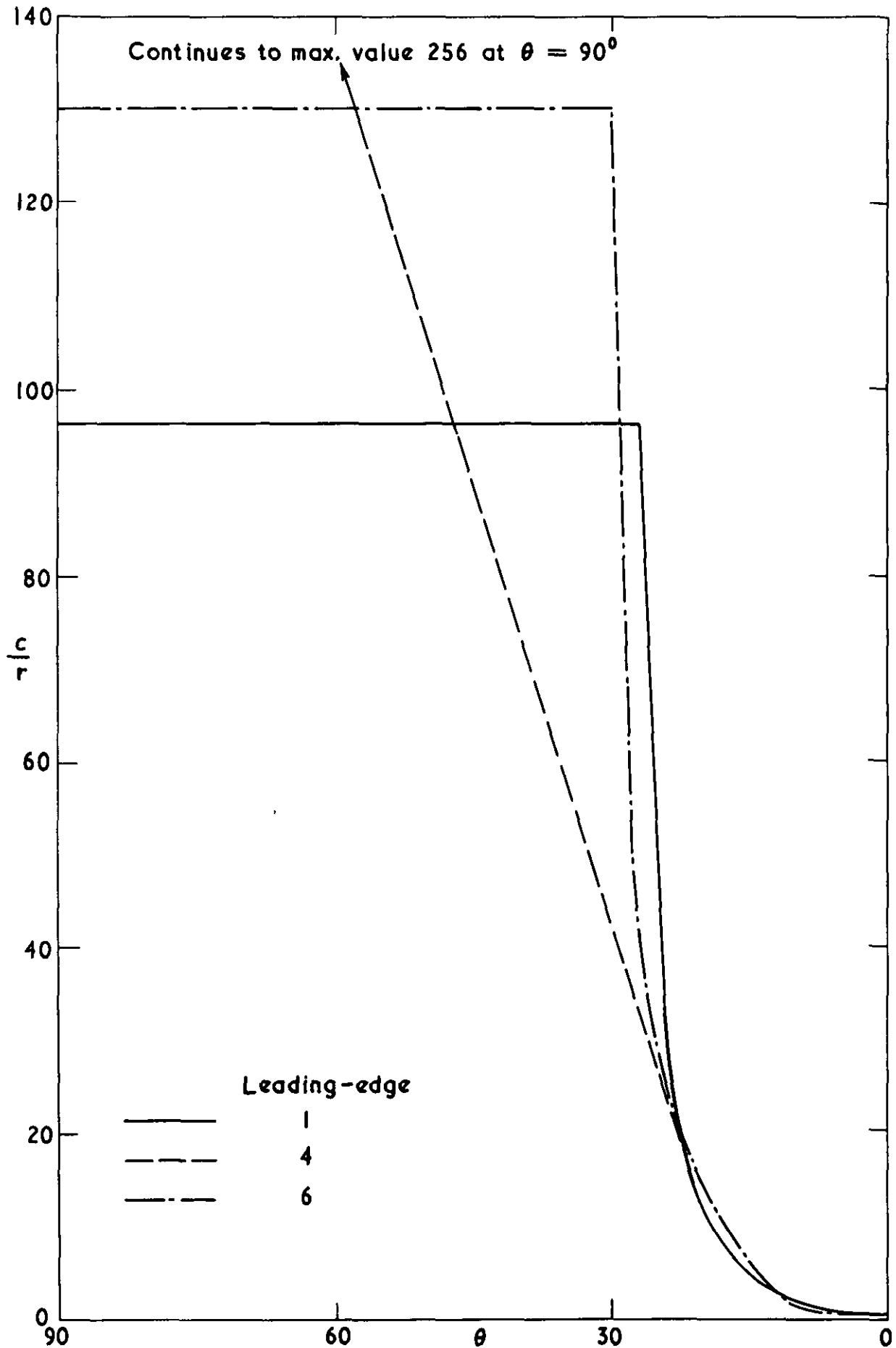
FIG. 1

	Leading-edge	N.P.L. Aerofoil No.
—	3	2 2 1 3
- - -	5	2 2 1 5



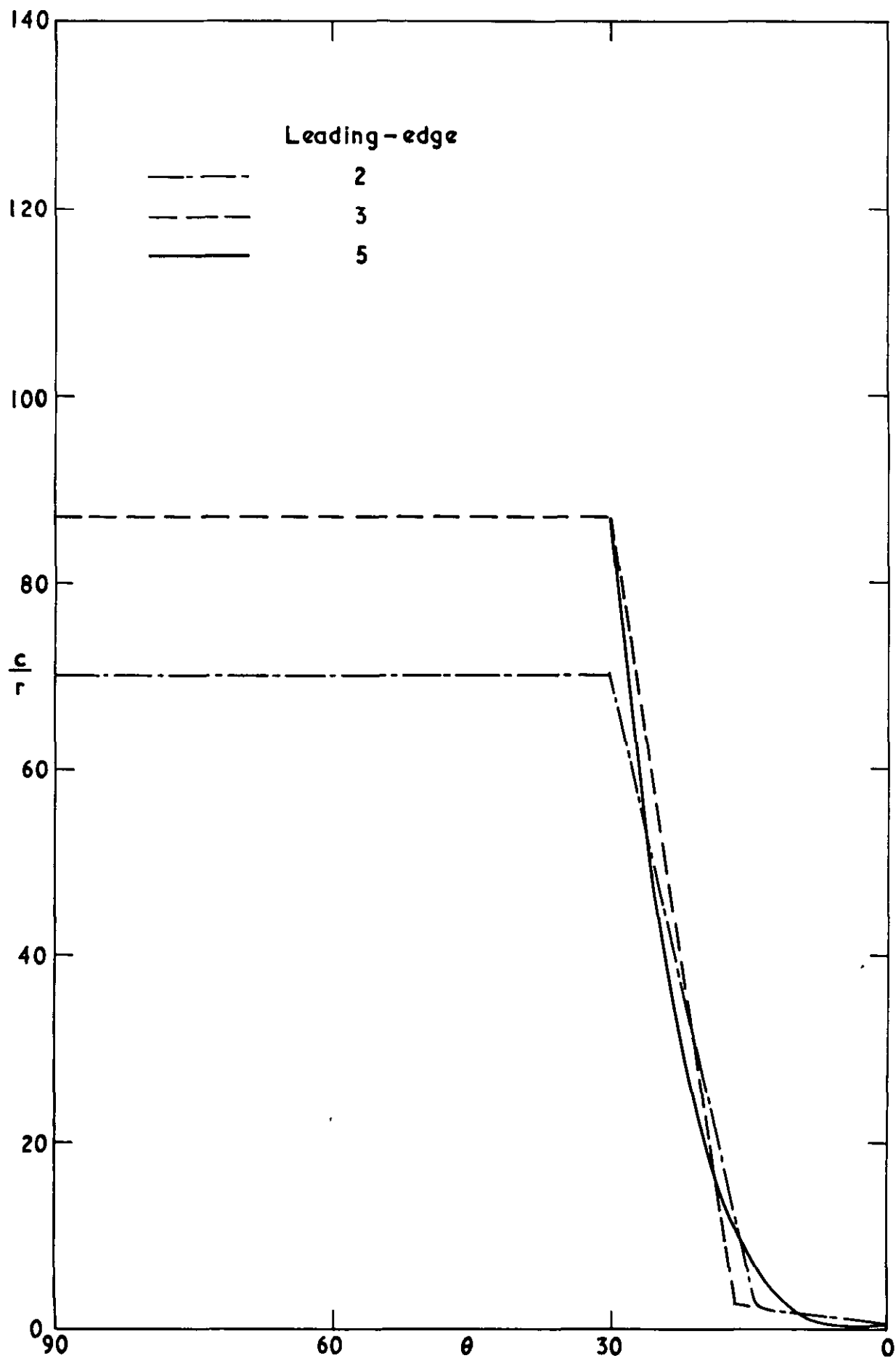
Comparison of profiles 3 and 5 (0 to 50% chord)

**FIG. 3**



Curvature distributions for profiles 1, 4 and 6

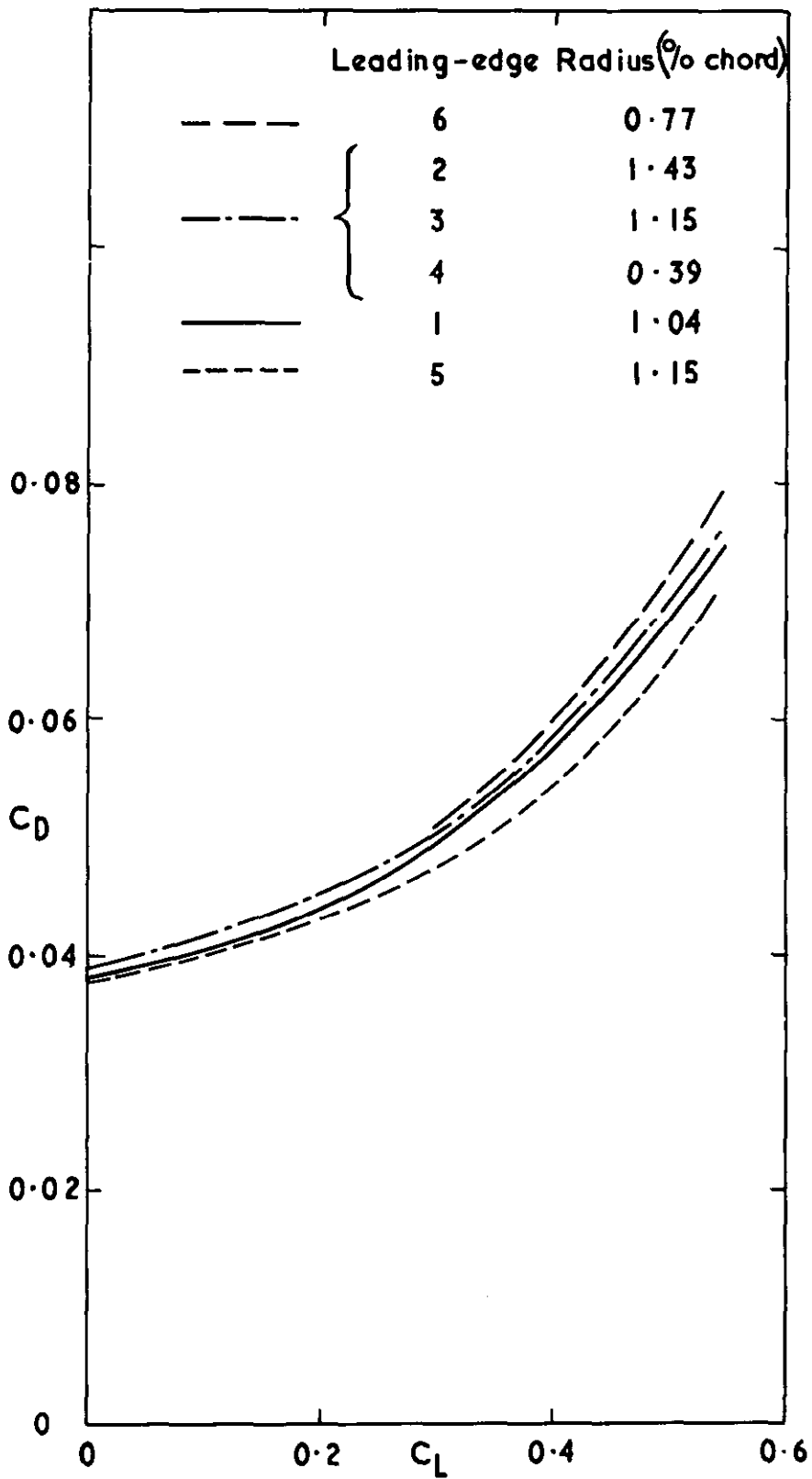
FIG. 4



Curvature distributions for profiles 2, 3 and 5

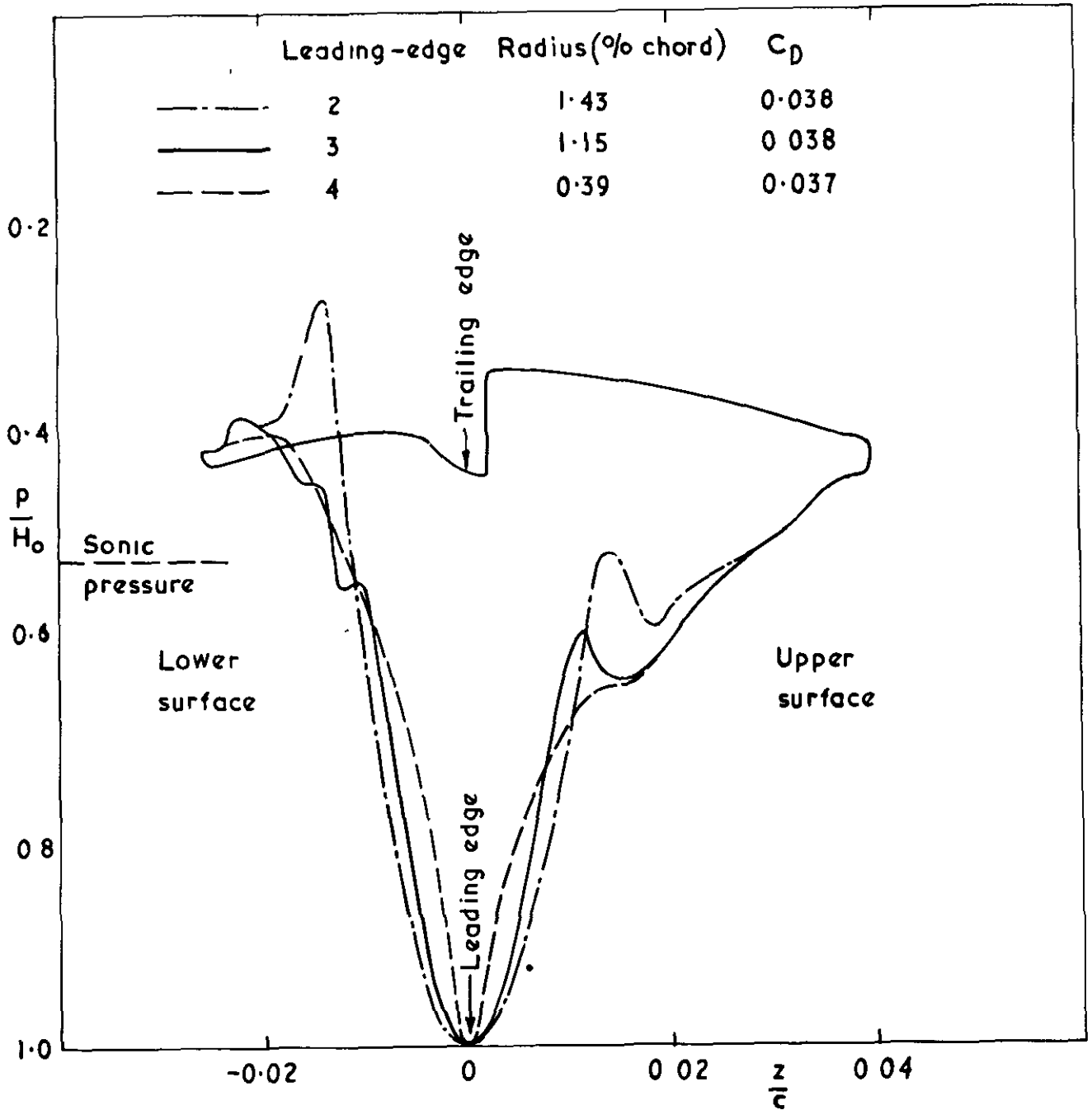


FIG. 5



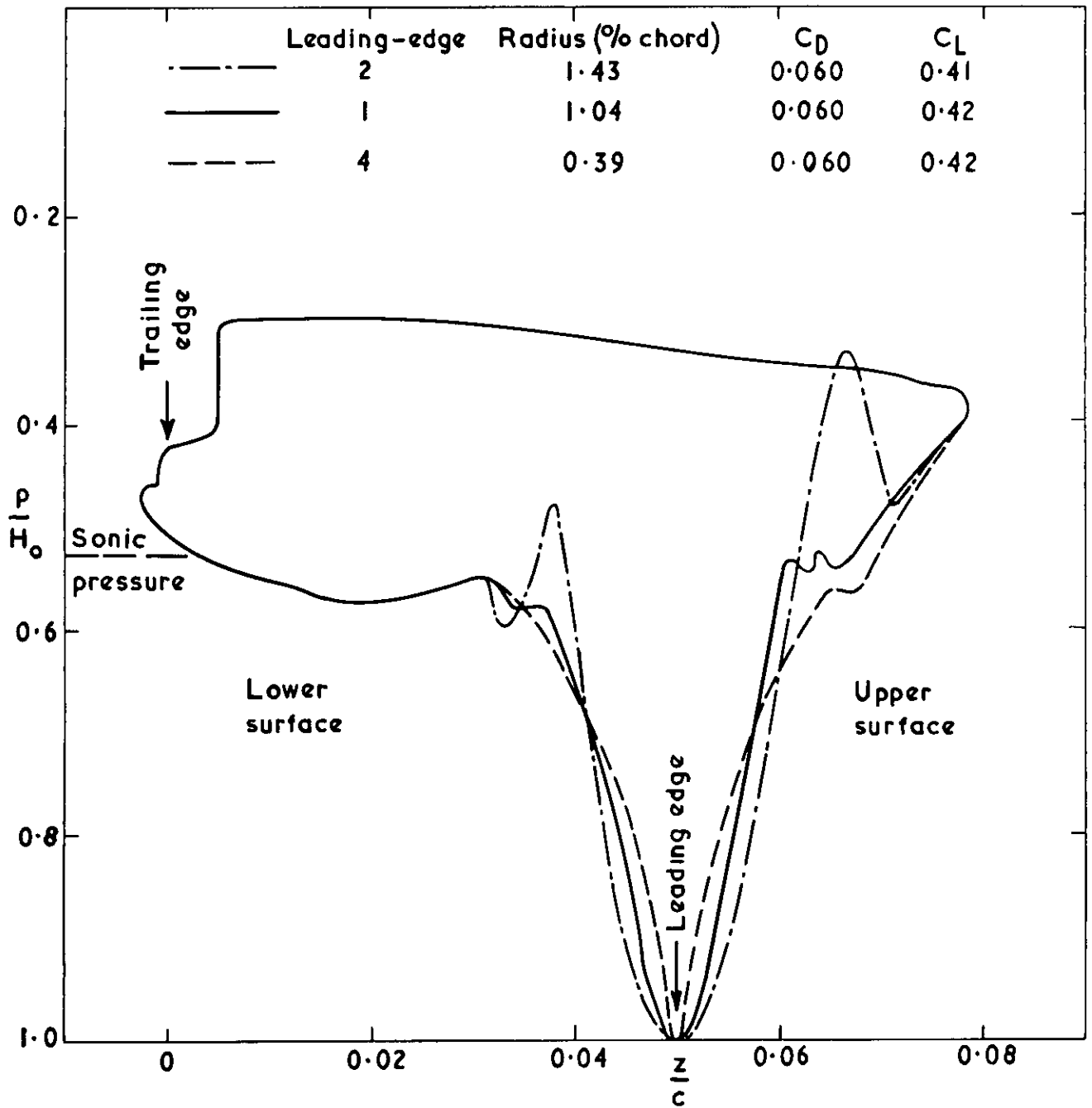
Drag coefficients as a function of lift coefficient at

$M_\infty = 1.0$



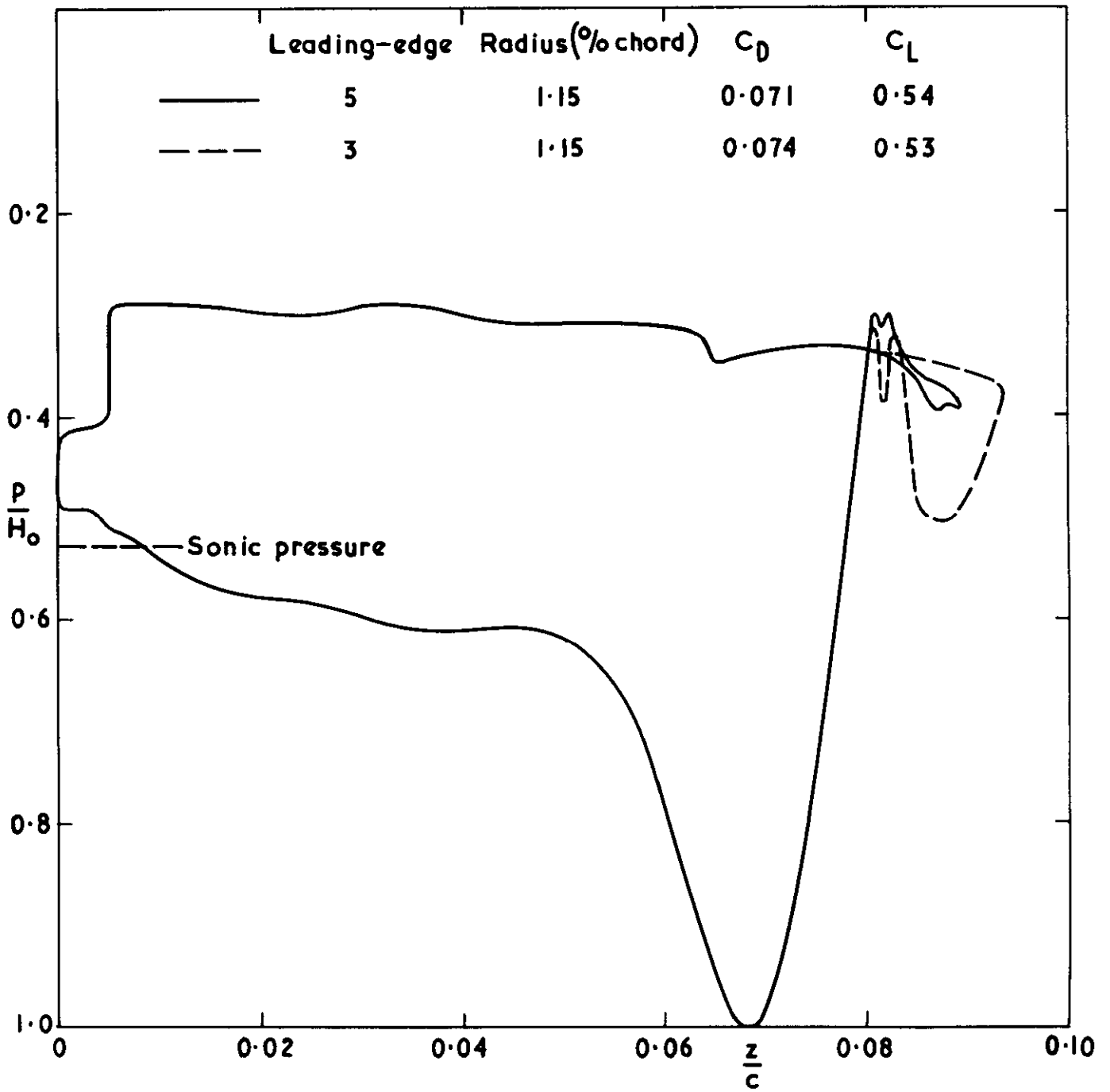
Pressure distributions at  $M_\infty = 1.0, \alpha = 0^\circ$

27 618  
FIG. 7



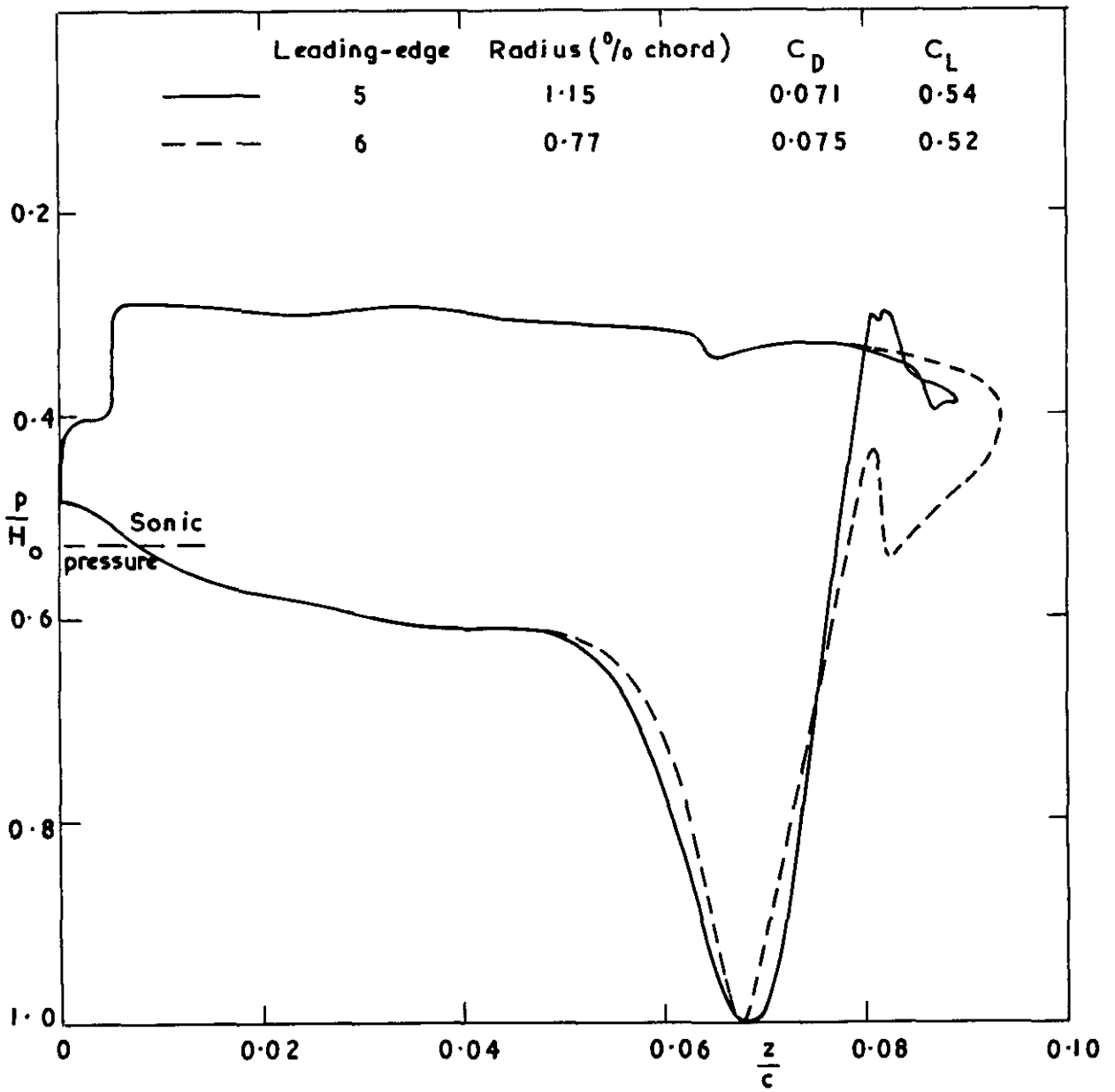
Pressure distributions at  $M_\infty = 1.0$ ,  $\alpha = 3^\circ$

**FIG. 8**



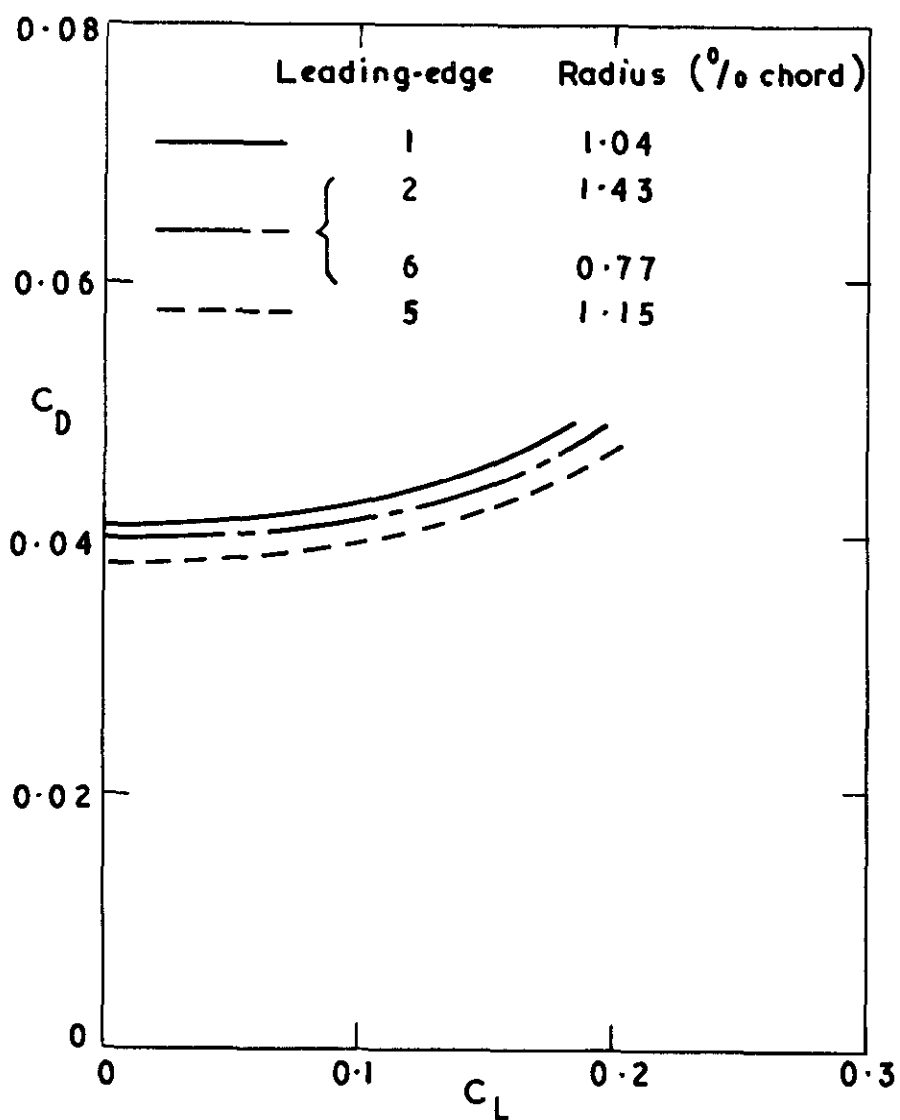
Pressure distributions at  $M_\infty = 1.0$ ,  $\alpha = 4^\circ$

FIG. 9



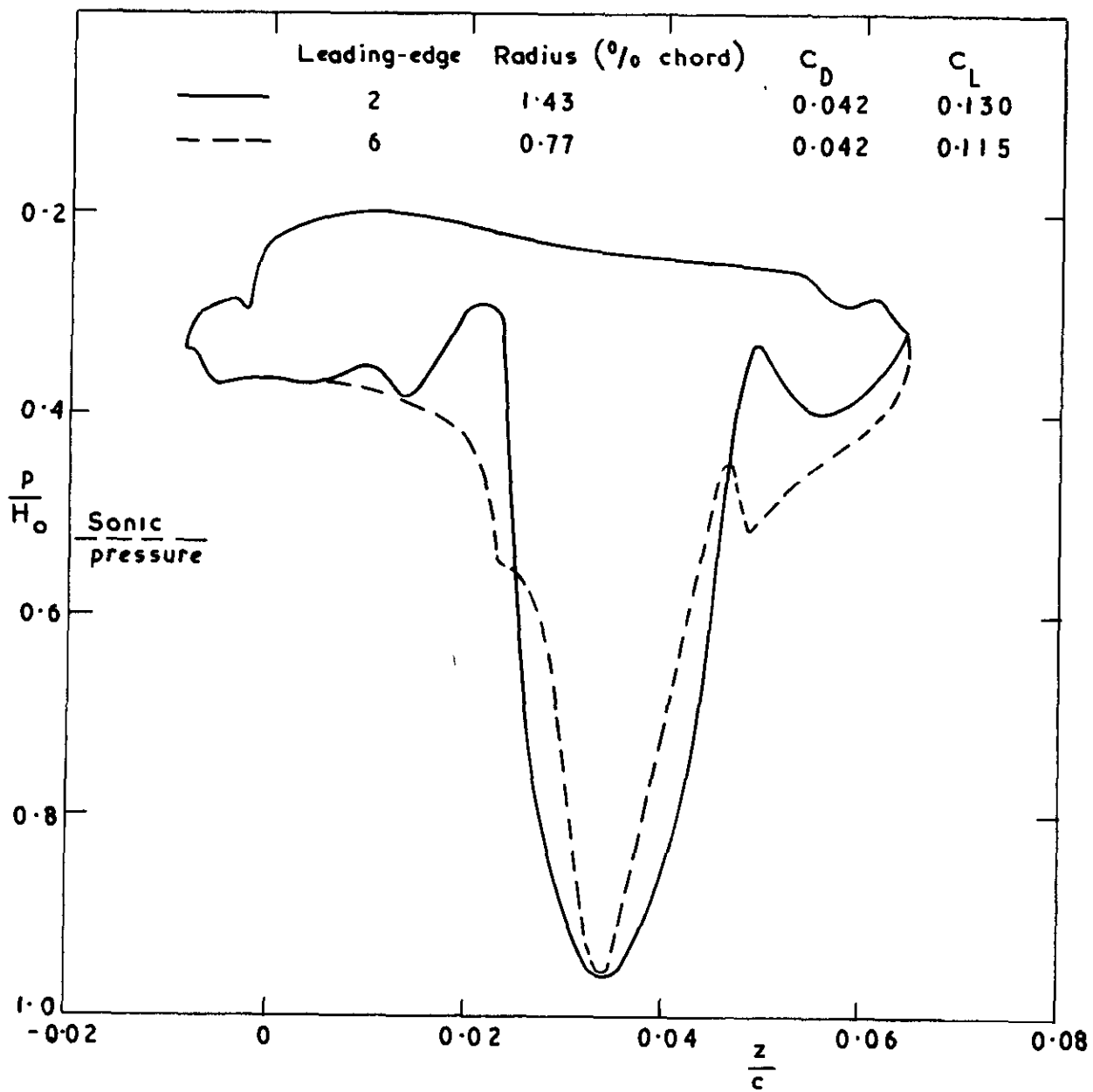
Pressure distributions at  $M_\infty = 1.0, \alpha = 4^\circ$

FIG.10



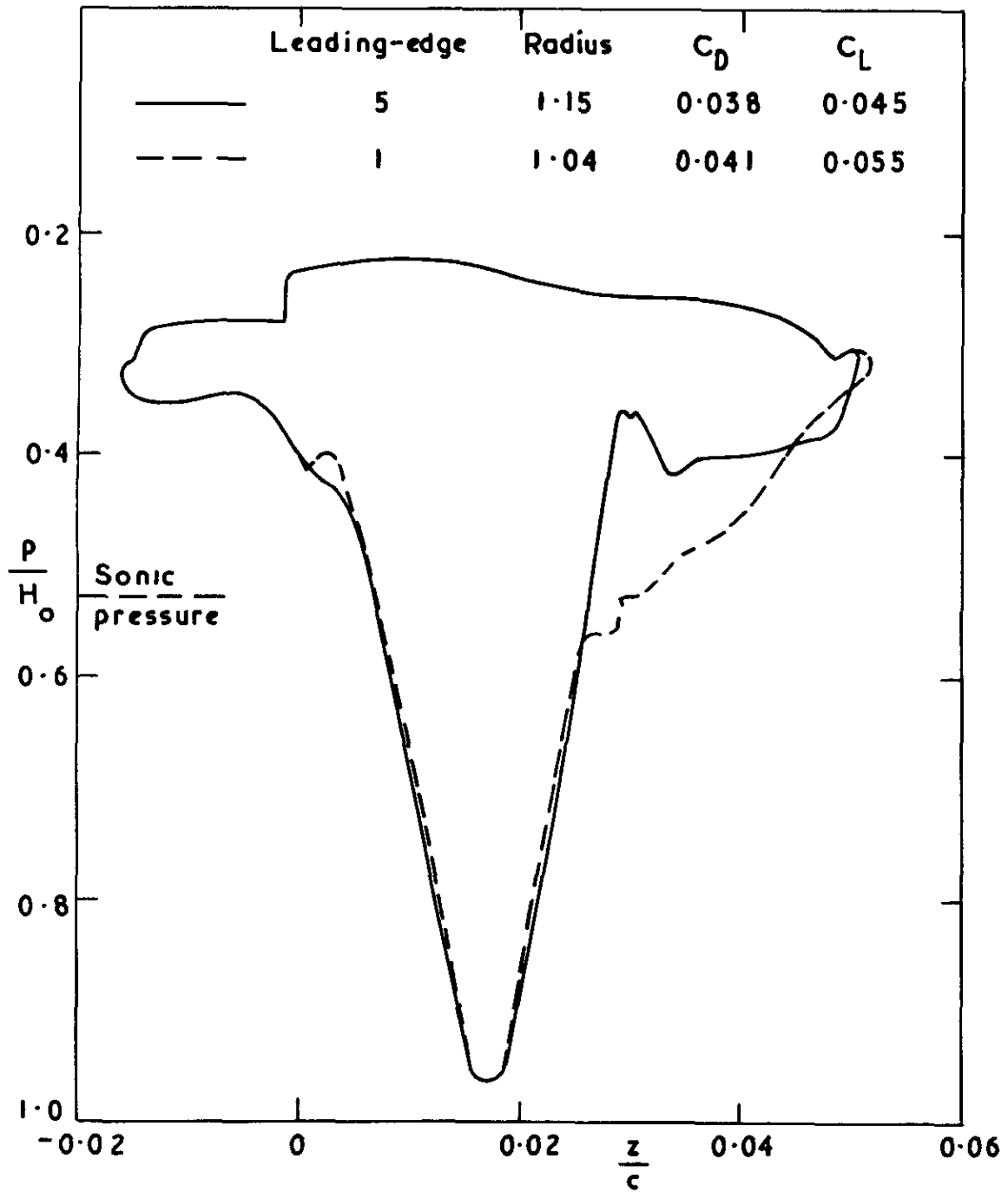
Drag coefficients as a function of lift coefficient at  
 $M_\infty = 1.4$

FIG.11



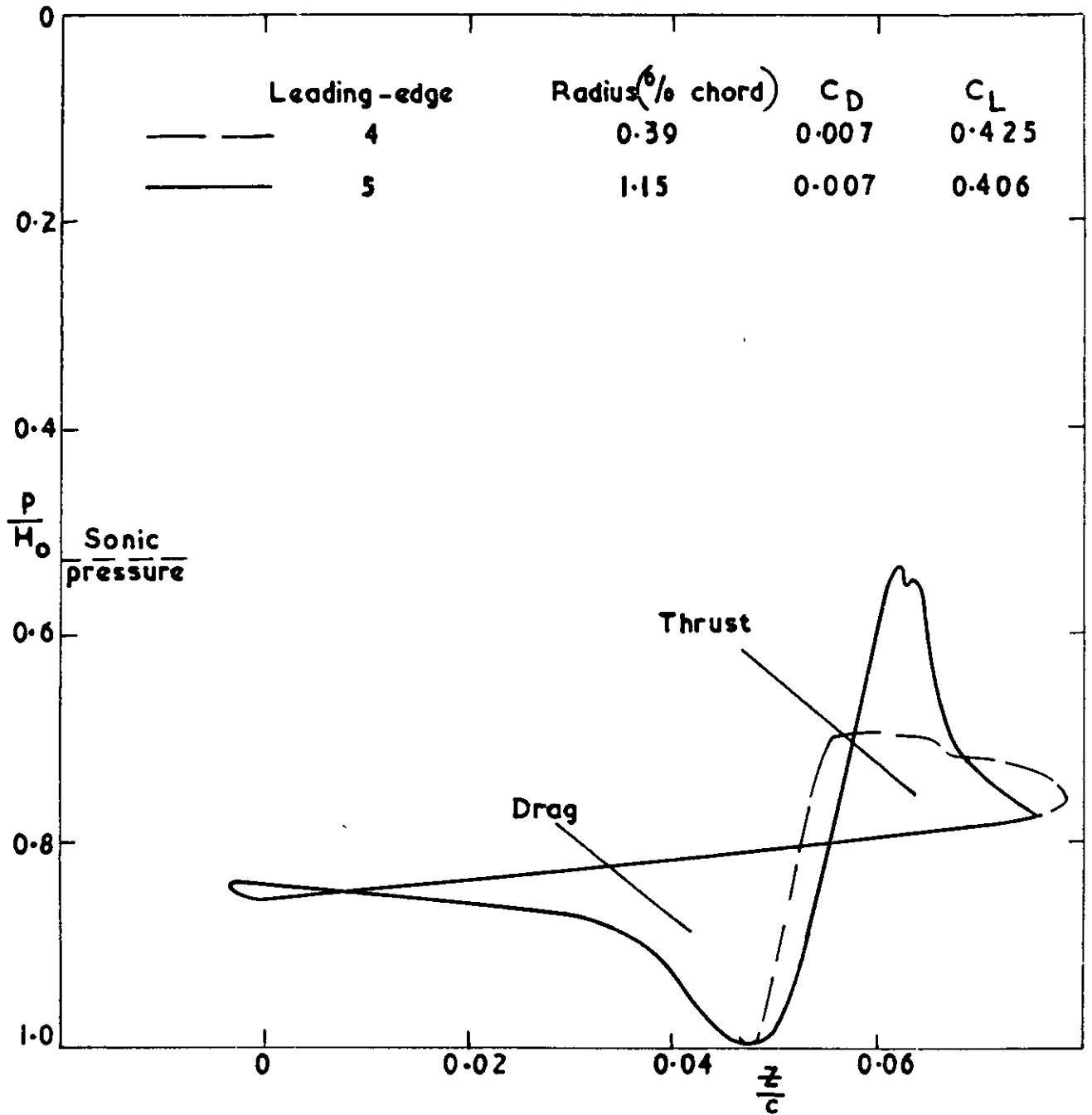
Pressure distributions at  $M_\infty = 1.4, \alpha = 2^\circ$

FIG.12



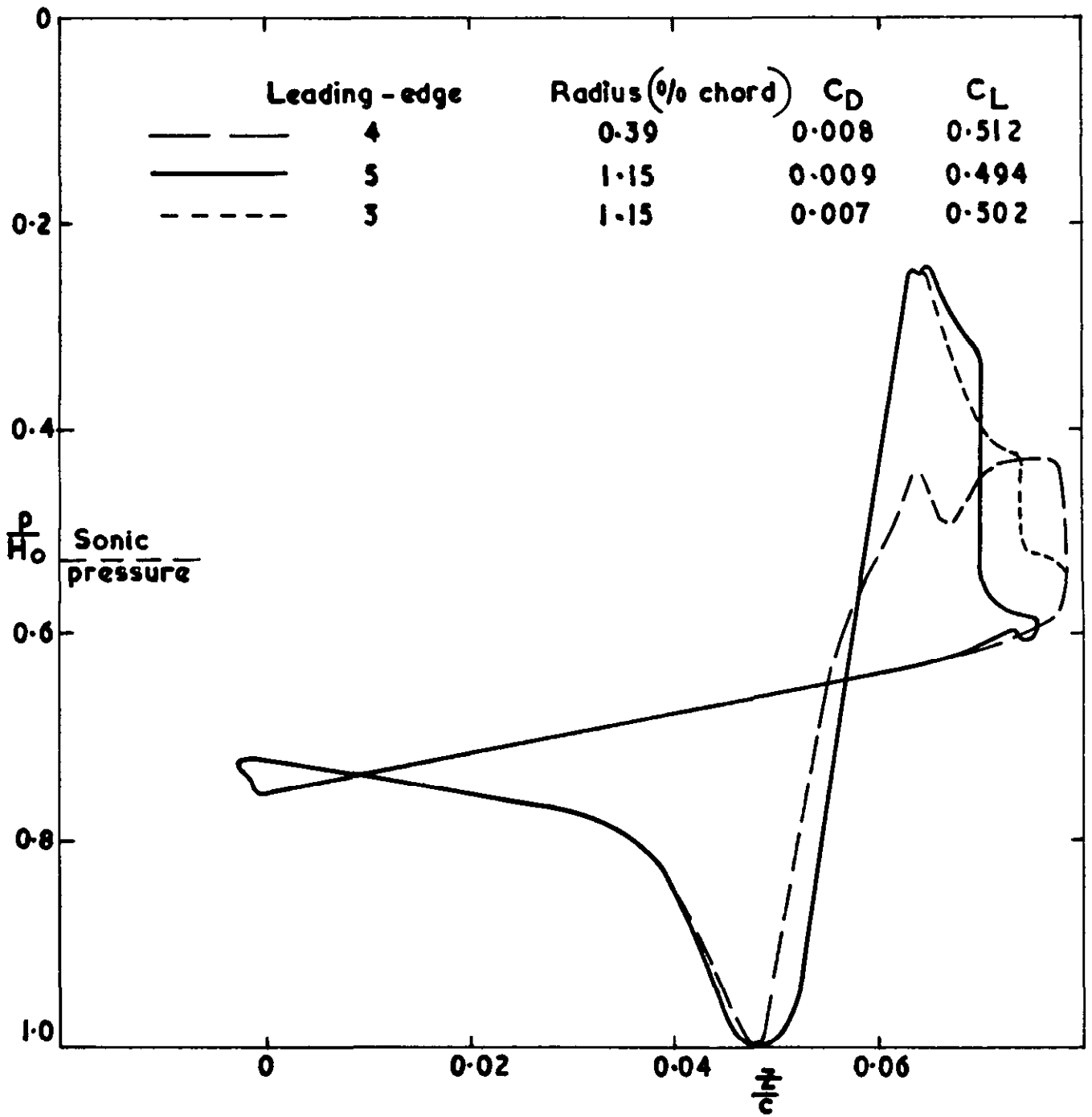
Pressure distributions at  $M_\infty = 1.4, \alpha = 1^\circ$





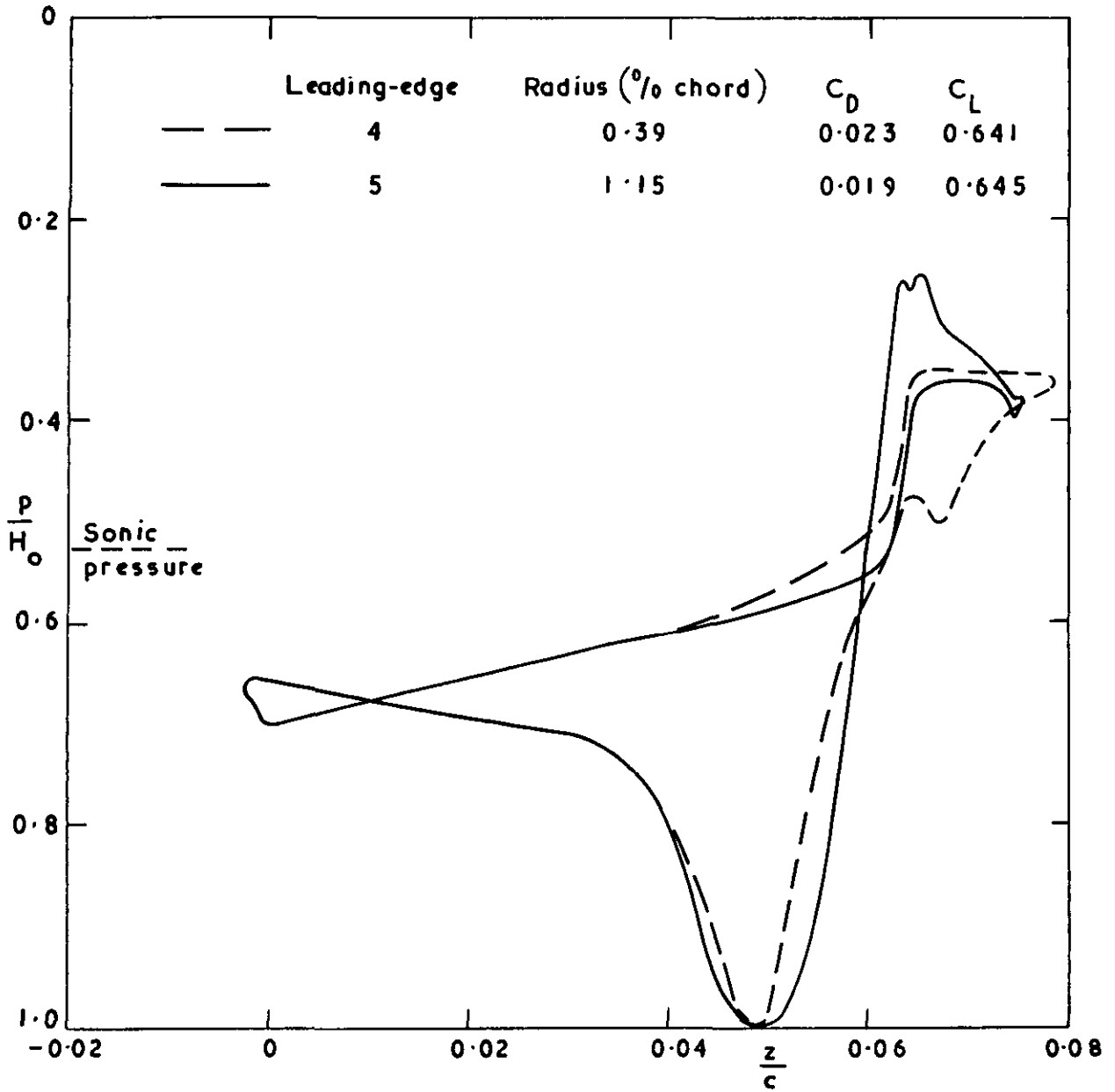
Pressure distributions at  $M_\infty = 0.5$ ,  $\alpha = 3^\circ$

FIG.14



Pressure distributions at  $M_\infty = 0.7$ ,  $\alpha = 3^\circ$

FIG.15



Pressure distributions at  $M_\infty = 0.8, \alpha = 3^\circ$



A.R.C. C.P. No. 921  
January, 1966  
Wilby, P. G.

THE PRESSURE DRAG OF AN AEROFOIL WITH SIX DIFFERENT ROUND  
LEADING EDGES, AT TRANSONIC AND LOW SUPERSONIC SPEEDS

The experimental pressure drags of a two-dimensional aerofoil are compared, for a wide range of leading-edge radii and other variations in curvature distribution, at transonic and low supersonic speeds. It is found that the drag does not increase with increasing leading-edge radius if the profile is designed so as to generate a rapid supersonic expansion. Furthermore, for a given radius, significant reductions in drag can be achieved by changing the way in which the leading-edge circle blends into the overall profile.

A.R.C. C.P. No. 921  
January, 1966  
Wilby, P. G.

THE PRESSURE DRAG OF AN AEROFOIL WITH SIX DIFFERENT ROUND  
LEADING EDGES, AT TRANSONIC AND LOW SUPERSONIC SPEEDS

The experimental pressure drags of a two-dimensional aerofoil are compared, for a wide range of leading-edge radii and other variations in curvature distribution, at transonic and low supersonic speeds. It is found that the drag does not increase with increasing leading-edge radius if the profile is designed so as to generate a rapid supersonic expansion. Furthermore, for a given radius, significant reductions in drag can be achieved by changing the way in which the leading-edge circle blends into the overall profile.

A.R.C. C.P. No. 921  
January, 1966  
Wilby, P. G.

THE PRESSURE DRAG OF AN AEROFOIL WITH SIX DIFFERENT ROUND  
LEADING EDGES, AT TRANSONIC AND LOW SUPERSONIC SPEEDS

The experimental pressure drags of a two-dimensional aerofoil are compared, for a wide range of leading-edge radii and other variations in curvature distribution, at transonic and low supersonic speeds. It is found that the drag does not increase with increasing leading-edge radius if the profile is designed so as to generate a rapid supersonic expansion. Furthermore, for a given radius, significant reductions in drag can be achieved by changing the way in which the leading-edge circle blends into the overall profile.

A.R.C. C.P. No. 921  
January, 1966  
Wilby, P. G.

THE PRESSURE DRAG OF AN AEROFOIL WITH SIX DIFFERENT ROUND  
LEADING EDGES, AT TRANSONIC AND LOW SUPERSONIC SPEEDS

The experimental pressure drags of a two-dimensional aerofoil are compared, for a wide range of leading-edge radii and other variations in curvature distribution, at transonic and low supersonic speeds. It is found that the drag does not increase with increasing leading-edge radius if the profile is designed so as to generate a rapid supersonic expansion. Furthermore, for a given radius, significant reductions in drag can be achieved by changing the way in which the leading-edge circle blends into the overall profile.





© *Crown copyright 1967*

Printed and published by  
HER MAJESTY'S STATIONERY OFFICE

To be purchased from  
49 High Holborn, London w c.1  
423 Oxford Street, London w.1  
13A Castle Street, Edinburgh 2  
109 St Mary Street, Cardiff  
Brazenose Street, Manchester 2  
50 Fairfax Street, Bristol 1  
35 Smallbrook, Ringway, Birmingham 5  
7 - 11 Linenhall Street, Belfast 2  
or through any bookseller

*Printed in England*